

Monte Carlo simulations of the new small-angle neutron scattering instrument SANS-1 at the Heinz Maier-Leibnitz Forschungsneutronenquelle

R. Gilles,* A. Ostermann and W. Petry

Technische Universität München, Forschungsneutronenquelle Heinz Maier-Leibnitz (FRM II), Lichtenbergstrasse 1, 85747 Garching, Germany. Correspondence e-mail: rgilles@frm2.tum.de

Received 14 August 2006
Accepted 6 February 2007

A new small-angle scattering instrument SANS-1 will be installed on beamline NL 4a at the Heinz Maier-Leibnitz Forschungsneutronenquelle (FRM II). It is a joint venture between the Technische Universität München and the Geesthacht Neutron Facility (GENF). SANS-1 has been optimized to be one of the most intense and versatile small-angle scattering instruments within the boundaries of available space and interaction with neighbouring instruments. Using the program *McStas*, the dimensions and the features of the different optical components were investigated and compared for the final selection. A vertical S-shaped neutron guide, a tower with two possible selectors, one for medium resolution at high intensity and one for high resolution, and two optimized transmission polarizers are the main advantages of SANS-1 compared with traditional instruments at other facilities.

© 2007 International Union of Crystallography
Printed in Singapore – all rights reserved

1. Introduction

To optimize a neutron scattering instrument to achieve ‘state of the art’ performance, many calculations and combinations of instrument component parameters have to be checked by Monte Carlo simulations in advance. The existing start position of the guide, the illumination of the guide with neutrons from the source and all the instrument components make complete Monte Carlo simulations necessary in order to consider the limitations and the options for the final set-up. The intensity, wavelength and divergence distribution are the main variables of the neutron beam which have to be followed through all neutron optics. Curvature, length and coating of neutron guides, beam cross section, choice of selector, positioning of neutron

optics, detector size and resolution *etc.* are typical parameters which have to be taken into account. Monte Carlo simulations allow us to analyse information about the instrument components which is often not available from experiments. The final choice of the set-up comes from a carefully chosen compromise between the flux and the resolution of the instrument.

All simulations were carried out with the program package *McStas* version 1.8 (Lefmann & Nielsen, 1999; Willendrup *et al.*, 2004). The standard guide component *Gravity_guide.comp* was taken from version 1.6 of the package because this component was tested in detail in former simulation work for different guide types. The gravity constant of this guide component was set to zero. In addition, for all instrument simulations the overall gravitation handling was switched off. For the neutron source the component *Source_gen.comp* was used. The wavelength spectrum of the cold source (Zeitelhack *et al.*, 2006) was modelled by three Maxwellian distributions. Based on the algorithm of the component *Gravity_guide.comp* from version 1.6, a component for the transmission polarizer was implemented.

2. Simulations of the S-shaped neutron guide

Fig. 1 shows a schematic drawing of the set-up of the new small-angle neutron scattering (SANS) instrument SANS-1. The beam hole SR1 faces the cold source and provides six neutron guides. Outside the reactor polygon a sixfold shutter for all six beamlines is positioned. After this shutter, beamline NL 4, 50 mm in width and 170 mm in height, is split into two: a 50 × 50 mm cross section beam (NL 4a) for SANS-1 on top and a 50 × 110 mm cross section beam (NL 4b) below for the prompt gamma activation analysis (PGAA) instrument. This arrangement allows us to bend the neutron guide of SANS-1 in the vertical direction and the neutron guide of PGAA in the horizontal direction for a single curved design.

The first step was to optimize a neutron guide system up to the position of the selector tower. This was done in such a way that a high

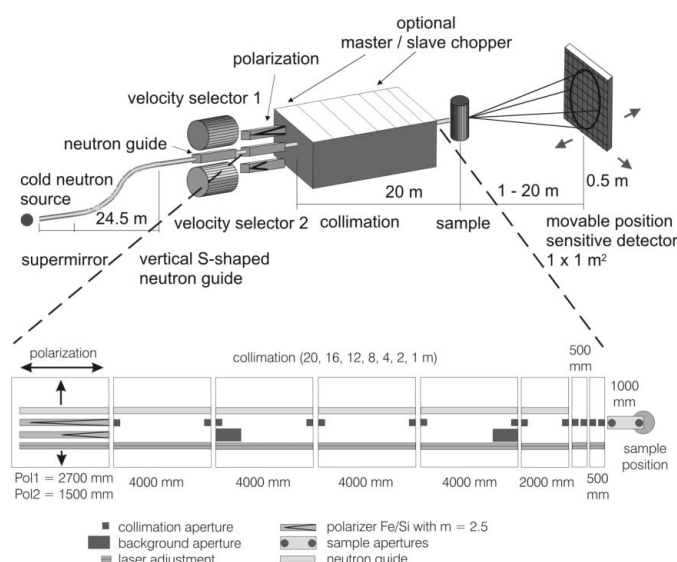


Figure 1
Schematic set-up of the new SANS-1 instrument at the FRM II.

neutron flux with low divergence in the wavelength range 4–30 Å will be transported. Additionally, undesired neutrons will be eliminated as much as possible in order to reduce the background. Single curved neutron guides have a disadvantage for SANS instruments at small wavelengths. Due to the different reflection probability of the inner and outer surface of the neutron guide, an intensity and divergence inhomogeneity results at the detector (Gilles *et al.*, 2006). As a consequence, isotropic patterns on the detector can not be effectively summed up by radial averaging.

To overcome these problems a vertical S-shaped neutron guide was built up. The basic idea of an S-shaped neutron guide is to shift the beam to a nearly parallel position without any significant change of the neutron distribution. Further, this guide gives a sharp cut-off for the small neutron wavelengths which cannot be used for experiments and otherwise would contribute to the background. Different bending radii of curvature and coatings were simulated to reach an optimized neutron guide configuration. For the simulations of different S-shaped and single curved guides for this 24.5 m section we used a polygonal set-up (108 pieces, component Gravity_guide.comp version 1.6). This allowed us to simulate guide systems which are bent simultaneously in both the horizontal and vertical direction (see below). Fig. 2 shows a comparison of flux and cut-off wavelength for different parameters of S-shaped neutron guides. For comparison, a typical single curved neutron guide is also shown in Fig. 2. Due to the limited space for the SANS-1 instrument, only a minimum curvature radius of 1000 m for a single curved neutron guide is feasible. Of particular importance, the sharp intensity cut-off for S-shaped neutron guides over four orders of magnitude at small wavelengths minimizes the background from short-wavelength neutrons. A slight inhomogeneity of the vertical intensity distribution is visible at the end of the collimation system if a neutron guide with a full cross section of 50 × 50 mm and no apertures are used in the collimation system. The inhomogeneity at the sample position will vanish if apertures are used in the collimation system.

More important is the symmetry achieved in the divergence profile which is not present in single curved neutron guides for small wavelengths (Gilles *et al.*, 2006) except when small apertures are installed in the collimation part. To implement further instruments in

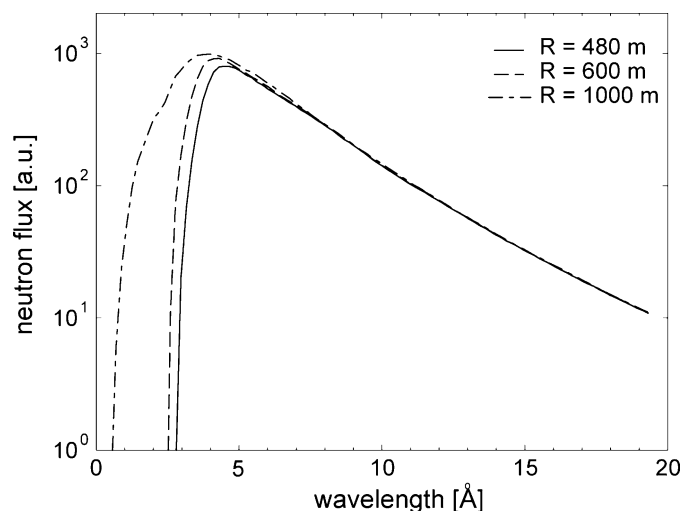


Figure 2 Neutron flux in arbitrary units (a.u.) at the sample position *versus* wavelength for two S-shaped neutron guides with different radii of curvature ($R = 480$ and 600 m) compared with a typical single curved neutron guide ($R = 1000$ m). In the collimation part a neutron guide of cross section 50 × 50 mm is used for the simulation.

the neutron guide hall, the vertical S-shaped guide has in the second part of the S-shape an additional horizontal curvature with a radius $R = 2100$ m and a length of 12.2 m. All subsequent parts of the instrument lie in a straight line. Simulations at the sample position show no significant loss in intensity (less than 2%) or influence on the divergence of the neutrons.

For the selection of the neutron guide parameters it was decided to fix the cut-off wavelength around 3 Å. The resulting curvature radius $R = 480$ m in the S-shaped part of the neutron guide shifts the neutron beam up by 300 mm to a final height of 1.57 m. A coating with $m = 2$ on the outer radius and $m = 1.2$ on the inner side of the curvature was revealed to be the best solution for high intensity with useful divergence (Fig. 2). Such a design allows us to install a supermirror ($m = 2$) on the top and bottom walls in the straight part before the S-shaped neutron guide to increase the intensity by around 13% at small wavelengths with tolerable divergence at the sample position. Owing to the fact that the inpile cross section is 170 mm in height and 50 mm in width, a better illumination of the top and bottom surfaces of the S-shaped part in the reduced 50 × 50 mm cross section is achieved.

This starting height of beamline NL 4a improves the flux at the sample position by around 8% compared with a horizontal S-shaped neutron guide. This horizontal configuration has a smaller illumination due to the geometry of the beam cross section at FRM II.

3. Simulations of various selector types

The typical useable wavelength range of a SANS instrument is between 4 and 20 Å. The difficulty of providing high resolution and simultaneously high intensity leads to the choice of the neutron velocity selector. Very often the decision is to use a so-called ‘standard selector’ with medium resolution at relatively high transmission. This standard selector is defined with 72 lamellae, a screwing angle of 48.3° and a maximum selector speed at 4.5 Å, resulting in a wavelength resolution with a full width at half maximum (FWHM) of around 10 to 11%, depending on the neutron beam cross section and the subsequent apertures used. SANS-1 is equipped with a selector tower with two possible selector positions and a third position for a neutron guide part to enable measurements with the white beam and the optional chopper system.

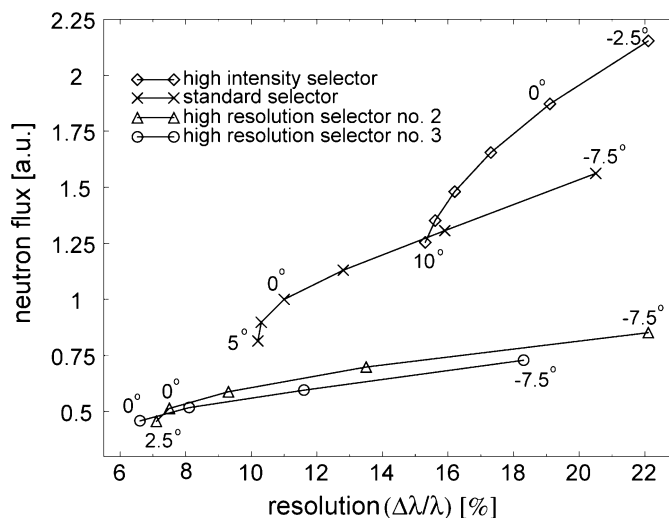


Figure 3 Neutron flux in arbitrary units (a.u.) just after the selector position *versus* selector resolution for four different ASTRIUM selectors calculated with adjusted selector frequency for different tilt angles. All simulations were done with a wavelength of 6.4 Å.

Table 1
Comparison of flux and resolution for different selectors.

Selector type	Specifications of ASTRIUM		Monte Carlo simulation with <i>McStas</i>					
	Analytical resolution $\Delta\lambda/\lambda$ (%)†	Accessible wavelength range (Å)	No. of lamellae	Screwing angle (°)	Relative flux (%) and resolution $\Delta\lambda/\lambda$ (%)†		Relative flux (%) and resolution $\Delta\lambda/\lambda$ (%)‡	
Standard	10.3	≥ 4.5	72	48.3	100	11.1	100	10.6
High intensity	18.4	≥ 4.5	45	42.9	186	19.2	189	18.6
High resolution No. 1	7.9	≥ 4.5	120	39.0	70	9.3	68	7.6
High resolution No. 2	6.2	≥ 5.6	144	42.9	52	7.5	50	6.1
High resolution No. 3	5.6	≥ 6.4	144	48.3	43	6.6	42	5.6

† Just after the selector, $\lambda = 6.0 \text{ \AA}$. ‡ At sample position for 6.0 \AA and tilt angle 0° (selector high resolution No. 3 is simulated for 6.4 \AA).

In the following, different selectors will be compared in terms of transmission and resolution on changing the number of lamellae, the screwing angle of lamellae and the possible tilting angles. For this comparison of different selectors the Monte Carlo simulations (component Selector.comp) include the wavelength distribution of neutrons from the cold source feeding beamline NL 4a and all neutron guide parameters including cross section, curvatures, coatings and gaps of neutron guide segments.

The collimation part described in Fig. 1 shows how the beam is collimated together with two optional sample apertures up to the sample position. Fig. 3 gives the relative neutron flux after the selector *versus* resolution for different types of selectors provided by the German company ASTRIUM. In general, resolution values of the selector up to 20% FWHM can be reasonable for special cases. Scattering curves detected with poorer resolution are strongly smeared and could not be evaluated. The combination of two selectors, one selector for very high resolution of about 6% FWHM and a complementary one for high intensity of about 20% FWHM, is not satisfying because both selectors have no acceptable intensity or resolution in the intermediate range even if they are tilted to change the resolution. Standard measurements with medium resolution of about 10–11% (as used by the majority of users in the community) receive no adequate transmission for the two selectors mentioned above. A selector of high intensity has no configuration for the accessible resolution in the range 10–11% FWHM while the selector for high resolution loses more than 50% of the intensity compared with a standard selector and high resolution selector with $\Delta\lambda/\lambda = 5.6\%$, where λ is the wavelength.

Another disadvantage that must be taken into account is the minimum accessible wavelength, of 6.4 \AA , of the high resolution selector. This restriction is due to the maximum selector rotation frequency (high resolution requires a higher number of lamellae, which means an increasing mass and consequently limitation of the rotation frequency). Wavelengths above 6.4 \AA can be used without any restrictions for such selectors. On the other hand, the transmission of the high intensity selector with 45 lamellae and 42.9° screwing angle is not much higher than for the standard selector. Therefore, as a first option, the standard selector has been ordered, while a second, high resolution, selector is foreseen as a future upgrade.

The different types of high resolution selectors, with a summary of the accessible wavelengths and resolution, are given in Table 1. The best resolution is reached by the selector called ‘high resolution No. 3’, which yields $\Delta\lambda/\lambda = 5.6\%$. Simulations were carried out with apertures of $50 \times 50 \text{ mm}$ in the collimation part and two apertures of 10 mm in diameter installed in front of the sample position.

Besides the Monte Carlo simulation, a second analytical calculation for the selector resolution was performed. The manufacturer, ASTRIUM, uses a simplified geometrical calculation for clients to figure out which selector choice is favourable. This simplification includes a maximum divergence for the incoming beam of the

selector; the real divergence distribution is not taken into account. An approximation for a ^{58}Ni neutron guide (horizontal coating of the S-shaped guide) is a divergence of $36'$ at a wavelength of 6 \AA . Including the parameters of the beam width of two adjacent lamellae and the neutron beam orientation due to the screwing angle of the selector, the selector resolution can be calculated (Table 1). A further simplification uses a Gaussian-shaped transmission function for the selector according to the calculations of a Soller collimator. Owing to these simplifications, a comparison of the analytical values and Monte Carlo simulations just after the selector shows the former gives more favourable results. If the resolution values of the Monte Carlo simulations are used, which is a more accurate description of the experimental case, the values obtained will be closer to the analytical results. Both of these statements are confirmed in Table 1. The small variations result from the slightly higher vertical divergence of the neutrons at the entrance of the selector because of the curved neutron guide, the neutron guide part with an $m = 2$ coating on the top and bottom walls before the S-shaped neutron guide, and how the cold source illuminates the initial part of the neutron guide.

Resolution values $\Delta\lambda/\lambda$ are calculated by using a beam of a certain maximum divergence and a simplified transmission function of the selector. The resolution is defined by

$$\Delta\lambda/\lambda = (\alpha^2 + \beta_o^2)^{1/2} / \text{tg}(\gamma) \quad (1)$$

(Friedrich *et al.*, 1989; Wagner *et al.*, 1992), where α is the divergence of the incoming beam (depending on the coating and curvature of the neutron guide), β is the divergence between two adjacent lamellae (depending on the distance between two lamellae and the rotor length) and γ is the angle between the incident neutron beam and the screwing of the lamellae (depending on the distance from the beam centre to the selector window position, the rotor length and the screwing angle of lamellae).

A meaningful comparison of different flux values after various selectors can only be done by Monte Carlo simulation, as this is the only method which fully considers all the parameters of the cold source, the wavelength spectrum and the real divergence distribution of the neutron beam.

4. Simulations of the polarizer concept

After passing the selector part, a collimation system with four parallel tracks will be installed and is now under construction (see Fig. 1). One track is occupied by a neutron guide, the second has apertures for improving resolution, the third position is for a laser system and the last one is equipped with background apertures and can also be used for newly developed optical components in the future. At the beginning of this assembly two transmission polarizers (cross section $50 \times 50 \text{ mm}$) are located. This type of transmission polarizer consists of two Si wafers coated on both sides with Fe/Si supermirrors ($m =$

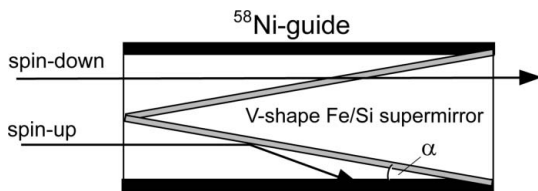


Figure 4
Schematic drawing of the transmission polarizer (top view). Two Si wafers with an Fe/Si supermirror coating are arranged in a V-shape set-up inside a ^{58}Ni guide. Spin-down neutrons are transmitted. Spin-up neutrons are reflected on the Fe/Si supermirror wafers and afterwards are absorbed in the glass wall of the ^{58}Ni guide.

2.5) which are placed in V-shaped set-up inside a ^{58}Ni neutron guide (see Fig. 4). The basic principle of this polarizer type is that the reflectivity curves of the Fe/Si supermirror wafers are different for the two spin components (Keller *et al.*, 2000). For one spin component (spin down in Fig. 4) the critical angle for total reflection is equal to the critical angle of the Si wafer ($\sim 0.06^\circ \text{ \AA}^{-1}$). For the other spin component (spin up in Fig. 4) the reflectivity curve depends on the m value of the Fe/Si supermirror. The spin-down neutrons are transmitted through the polarizer due to the low reflectivity and the chosen gradient angle α of the Fe/Si supermirror wafers with respect to the neutron beam. Because of the higher reflectivity, spin-up neutrons are reflected thus increasing their divergence by two times the angle α of the Fe/Si supermirror wafers with respect to the incoming beam. In most cases, these neutrons cannot be reflected at the outer ^{58}Ni guide. They are transmitted through the ^{58}Ni coating and are absorbed.

The advantage of this device compared to the conventionally used polarization bender devices is that the neutron beam is not deflected. The gradient angle of the Fe/Si supermirror wafers (and therefore the length of the transmission polarizer), the m value of the Fe/Si

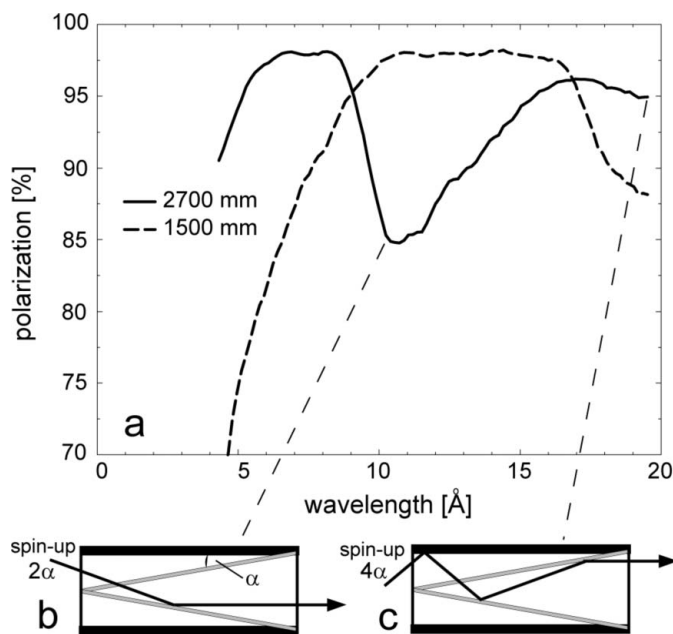


Figure 5
(a) Polarization of a 2700 mm ($\alpha = 0.53^\circ$) and a 1500 mm ($\alpha = 0.95^\circ$) long V-shaped Fe/Si transmission polarizer ($m = 2.5$) versus wavelength at the sample position. The set-up implies 19 m collimation with apertures of 50×50 mm. (b) and (c) show schematically the reason for the polarization breakdown. (b) Spin-up neutrons with a divergence of two times the gradient angle α of the Fe/Si supermirror wafers. (c) Spin-up neutrons with a divergence of 4α .

supermirror and the outer guide were the subject of the Monte Carlo simulations. Fig. 5 shows the simulation results of the two optimized Fe/Si transmission polarizers. When the full collimation path is used, a polarization breakdown can be observed depending on the gradient angle α of the Fe/Si supermirror wafers. Depending on the wavelength and divergence of the incoming neutrons it is possible for neutrons with the wrong spin orientation (here spin up) to be reflected on the inner side of the 'V' after transmission (see Fig. 5). If the divergence of the incoming neutrons is 2α or 4α , then the final divergence will be around 0° (parallel to the direction of the neutron guide). These neutrons can reach the sample position. In this case, the polarization drops for a broader gap of wavelength before the polarization increases to higher values again. To fill this polarization gap a second V-shaped polarizer has to be used. Therefore, the final choice consists of two transmission polarizers with lengths 2700 mm ($\alpha = 0.53^\circ$) and 1500 mm ($\alpha = 0.95^\circ$), respectively. The optimum m value of the Fe/Si supermirror is $m = 2.5$. With the full collimation length a polarization of at least 95% over a wavelength range from 5 to 17 \AA can be achieved. With decreasing collimation length the polarization decreases to a value of about 91%.

Additional elements such as lenses and a spin flipper or possibly focusing supermirrors are foreseen for the collimation unit. The set-up of the collimation unit allows the possible addition of a chopper system, with a master and two slave choppers, to be implemented at a later date.

The detector tube of around 2.8 m in diameter allows the use of an area detector of 1×1 m with lateral movement up to 0.5 m. This gives benefits in two ways. The Q range is expanded to higher Q values due to the larger accessible solid angle [$Q = (4\pi/\lambda)\sin\theta$, where 2θ is defined as the scattering angle]. Provided isotropic scatterers are studied, the asymmetric detector positions allow one to minimize the necessary number of sample-to-detector positions for a required Q range. Normally the detector pixel resolution of 8–10 mm is sufficient for a SANS instrument because other resolution parameters have stronger contributions.

5. Conclusions

A vertical S-shaped neutron guide improves the selection of useful neutrons by a sharp wavelength cut-off for small wavelengths and provides a homogenous neutron distribution in intensity and divergence at the sample position for all wavelengths. Consequently, it is expected to decrease the background of the instrument compared with a single curved neutron guide. The choice of two possible selectors provides a more flexible method for improving the resolution for special applications and the opportunity to insert the replacement selector quickly. Another important advantage of this concept is the beam height (1.57 m), which allows higher flexibility for different sample environments. The optimization of two transmission polarizers can provide a high polarization of $\geq 95\%$ for a broad wavelength range from 5 up to 17 \AA . A large 1×1 m area detector with a spatial resolution of 10 mm or less can also be accommodated.

We thank the authors of *McStas* (in particular K. Lefmann, K. Nielsen and P. Willendrup) for providing the program and fruitful discussions, P. Link for providing the selector component, and R. Kampmann and A. Schreyer from GENF for fruitful discussions.

References

Friedrich, R., Wagner, V. & Wille, P. (1989). *Physica B*, **156–157**, 547–549.

conference papers

- Gilles, R., Ostermann, A., Schanzer, C., Krimmer, B. & Petry, W. (2006). *Physica B*, **385–386**, 1174–1176.
- Keller, T., Krist, T., Danzig, A., Keiderling, U., Mezei, F. & Wiedenmann, A. (2000). *Nucl. Instrum. Methods Phys. Res. A*, **451**, 474–479.
- Lefmann, K. & Nielsen, K. (1999). *Neutron News*, **10**(3), 20–23.
- Wagner, V., Friedrich, H. & Wille, P. (1992). *Physica B*, **180–181**, 938–940.
- Willendrup, P., Farhi, E. & Lefmann, K. (2004). *Physica B*, **350**, 735–737.
- Zeitelhack, K., Schanzer, C., Kastenmüller, A., Röhrmoser, A., Daniel, C., Franke, J., Gutschiedl, E., Kudryashov, V., Maier, D., Päthe, D., Petry, W., Schöffel, T., Schreckenbach, K., Urban, A. & Wildgruber, U. (2006). *Nucl. Instrum. Methods Phys. Res. A*, **560**, 444–453.